第 44 卷 第 9 期/2024 年 5 月/光学学报 研究论文

光学学报

基于微光纤尖端激光脉冲推进微球

邢继伟，孙文慧，刘雪连，刘艳芬，刘晓华，刘晓军，郝斌政，李建军，罗旺，李奇楠，于海超*

齐齐哈尔大学理学院物理系，黑龙江 齐齐哈尔 161006

摘要 本文研究了基于锥形光纤结构的激光推进微球，并基于该结构探究推进机制、微球运动的影响因素。光纤尖端出射的激光能量超过空气的电离阈值而产生等离子体，随后等离子体膨胀形成的冲击波通过反冲作用驱动微球。结果表明，微球的推进冲击波弹射机制发挥了主导作用。研究了激光能量和微球直径对微球运动的影响，发现微球的运动距离依赖于光纤尖端出射激光能量和微球尺寸。此外，分析了光纤尖端尺寸对激光能量、能量密度的影响，揭示出尖端出射激光能量呈非线性增加，能量密度表现出相反的变化趋势。该研究可能为在微米水平上对胶体和生物物质的指令操作提供更多的理论支撑。

关键词 激光；锥形光纤；等离子体；脉冲；冲击波

中图分类号 O439 **文献标志码** A **DOI**：10.3788/AOS231931

1 引 言

激光推进过程中，激光撞击靶材表面，周围的空气或靶材表面物质电离，形成等离子体[1-2]。随后等离子体膨胀形成的冲击波压力通过反冲作用施加到靶材表面，实现动量的转移。等离子体的形成、冲击波的后续演化以及动量传递是研究激光推进机制的基本问题。揭示激光推进本质的是激光与靶材的相互作用[3-6]。相比于传统的化学燃料推进，激光推进不需要携带额外的燃料或推进剂（可以从目标本身或周围环境中获取），从而大大提高了推进效率[7-8]。

迄今为止，关于激光推进过程和条件的研究已有50年的历史。1972年，Kantrowitz[9]首次提出激光推进的概念，可以代替化学燃料推进，将航天器送入近地轨道。随后超高激光系统出现，并迅速应用于激光推进的实践中。Myrabo等[10]使用功率为10 kW的激光，成功地将质量为50 g、直径为12.2 cm的飞行器推进到71 m的高度。Klein等[11]证明激光撞击液体颗粒后，可导致颗粒产生移位和形变。张楠等[12]利用飞秒激光推进微珠，发现微珠可以在等离子体通道中稳定前进。王谦豪等[13]阐述了等离子体通道由自聚焦效应与散焦共同作用产生。Demos等[14]研究了金属粒子与纳秒激光的相互作用，阐述了激光与物质之间的相互作用机制。但是上述研究聚焦于高能激光直接照射靶材，靶材表面可能会受到永久性的损伤。此外，对于微小粒子的推进，激光光斑较大，易造成微粒运动轨迹偏移。因此，需要提出一种能够降低粒子表面损伤且能够控制激光光斑尺寸的装置。

微光纤表面的电磁场极强，可用于有效操纵粒子[15-19]。粒子受到足够大的辐射压力，从而沿着导波推进。考虑到微米甚至纳米锥形光纤能够传输激光，并且可以通过机械运动对进入[20-21]和离开[22]的激光做出响应，这为研究激光与电介质材料相互作用中的动量转换提供了一种可行的方法。在之前的研究中[23]，由锥形光纤尖端的激光脉冲推进单个玻璃微球，微球运动轨迹沿直线运动，但运动机制尚不清楚。因此，本文研究了基于锥形光纤结构的激光推进，该结构能够有效降低激光能量，且控制激光光斑大小。通过调整光纤尖端与微球中心的相对位置，记录微球动力学过程，发现微球可沿光纤方向及对角方向运动，证明激光推进过程中冲击波弹射机制发挥了主导作用。此外，研究还发现微球的运动距离与激光能量、微球尺寸以及锥形光纤尖端直径有关。基于光纤的弯折特性，本文研究为微观领域的激光定向推进提供了参考依据。

2 实验装置

微球运动的实验装置以及制得的锥形光纤如图1所示。锥形光纤尖端通过火焰加热锥形拉伸技术制得[24]。在制作过程中需要对光纤提前预热，目的是降低制得锥形光纤出现气泡或裂纹的风险。实验过程中

收稿日期：2023-12-14；**修回日期**：2024-02-06；**录用日期**：2024-02-23；**网络首发日期**：2024-03-13

基金项目：国家自然科学基金（61775044）、黑龙江省高校基本科研业务费（135509218，145109309，145209133）、博士研究启动基金（340279）

通信作者：*1240082167@qq.com

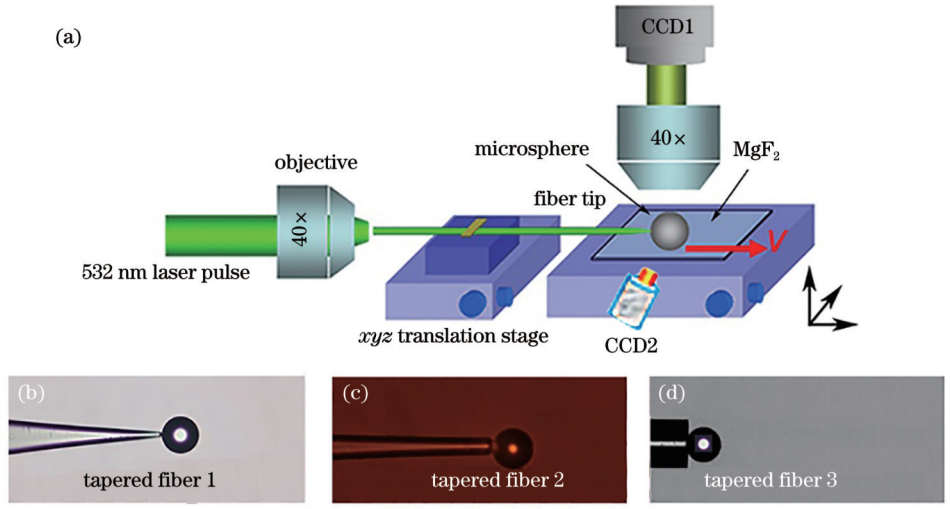

图 1　尖端出射的激光脉冲推进微球实验。(a)实验装置示意图;(b)~(d)光纤尖端尺寸分别约为 1.9、10、125 μm

Fig. 1　Experiment on laser pulse emitted from tip propelling microsphere. (a) Schematic diagram of experimental setup; (b)-(d) fiber tips with diameters of about 1.9, 10, and 125 μm, respectively

使用的玻璃微球通过传统熔融法制得[25]。实验中,使用倍频 Nd:YAG 激光(λ=532 nm,脉宽为 10 ns)作为激发光源,并且经 40×物镜耦合到光纤中。在光学显微镜下,用捕获光纤探针将制得微球直接沉积在 MgF_2 基质(折射率~1.39,表面粗糙度小于 0.2 nm)表面。锥形光纤尖端与微球的相对位置则是通过 x-y-z 位移平台灵活操纵(分辨率为 100 nm)。激发光沿着光纤继续传播经锥形光纤尖端出射,出射的激光能量将周围空气击穿并产生空气等离子体,随后膨胀形成冲击波驱动微球前进。微球表面的反射光经光学显微镜进入到相机 CCD1 中,用来记录微球的动力学过程。此外,通过竖直方向的相机 CCD1 与水平方向的相机 CCD2 的结合,确保锥形光纤尖端与微球的中心对齐,使微球沿锥形光纤方向运动。推进实验完成后,通过高性能光能量计[26-27]对光纤尖端出射激光能量进行测量。

3　实验结果与分析

3.1　基于锥形光纤结构推进机制的研究

选取尖端直径~8 μm 的锥形光纤、直径~80 μm 的微球进行推进实验。时间间隔为 1/1000 s 的相机 CCD1 用来捕捉微球的动力学过程[图 2(a)]。1/1000 s 后,CCD1 捕捉到从光纤尖端射出的激光,微球发生运动,且具有最大初速度。在 t=7/1000 s 时直线运动距离 s ~547 μm[图 2(b)~(h)]。微球停止后,能量计测量光纤尖端出射的激光能量 E ~9.6 μJ。

已知微球的密度 ρ=2.51 g/cm^3,质量 m≈6.7×10^{-10} kg。根据实验结果,在 t=2/1000 s 和 t=3/1000 s 时微球的运动距离分别为 S_c≈63 μm 和 S_d≈178 μm[图 2(c)~(d)],并且平均速度 v_c~11.5 cm/s。设运动过程中,微球与基质之间的阻力为 f。根据能量守恒定

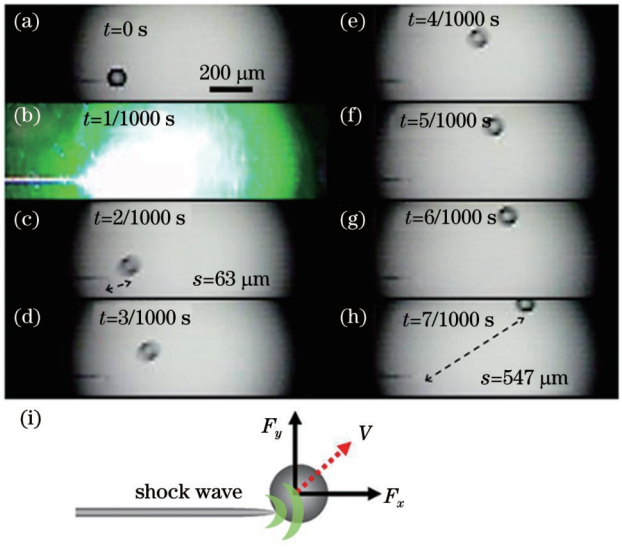

图 2　单激光脉冲推动微球的运动过程,锥形光纤尖端出射的脉冲能量~9.6 μJ。(a)~(h)微球运动轨迹的图像,其中时间间隔为 1/1000 s;(i)光纤尖端与微球中心相对位置示意图

Fig. 2　Motion process of microsphere propelled by single laser pulse, and energy of pulse coming out from tapered fiber tip is ~9.6 μJ. (a)-(h) Images of moving trace of microsphere, and time interval is 1/1000 s; (i) schematic diagram of relative position of fiber tip and center of microsphere

律,计算出阻力 f=1.2×10^{-8} N。微球在 t=1/1000 s 时应具有最大速度 v_{max},其计算公式为

$$v_{max}=\sqrt{\frac{2fS_c}{m}+v_c^2}。\tag{1}$$

从而计算出 v_{max} 为 12.4 cm/s,动量 P=mv_{max}=8.3×10^{-11} Ns。由于在实验中微球是沿着 MgF_2 基质表面滑动的,因此未使用 Stokes 公式来计算阻力。理论上,根

据 Brevik[28]的研究报道，介质中的动量密度为 $P_M=n\varepsilon/c=4.7\times10^{-14}$ Ns，其中 n 为光纤的折射率，ε 为介电常数，c 为光在真空中的速度。经对比，P 比 P_M 大约1000倍，由此说明在实验中微球的动力不来源于辐射压力。之前的研究表明[29]，由于激光在光纤尖端聚焦，能量密度达到空气的击穿阈值，空气被电离形成高温、高压的空气等离子体，随后膨胀形成以球形向外传播的冲击波，通过反冲作用驱动微球前进，并且随着激光能量的增加，冲击波施加在微球表面的作用力越大。即微球的推进过程中冲击波弹射机制发挥主导。此外，为进一步验证冲击波弹射机制发挥的主导作用，实验中通过 x-y-z 位移台将光纤尖端与微球中心偏移，结果发现微球沿对角方向运动，说明微球受到沿对角方向的作用力，与之前研究中阐述的冲击波呈球形向四周传播的结论相统一[图 2(i)]。

3.2　激光脉冲能量、微球尺寸对微球推进的影响

首先，在光纤尖端直径约为 20 μm 情况下，控制微球直径约为 40 μm，研究能量约为 3.5 μJ 和 25 μJ 时对微球运动的影响。结果表明，微球的运动距离随着激光能量的增加而增加。对应微球运动距离分别约为 45.4 μm 和 795.7 μm。这是由于随着激光能量的增加，等离子体膨胀形成的冲击波携带的能量增加，施加在微球表面的作用力增大。其次，在能量约为 25 μJ 时，研究微球尺寸对微球运动的影响。结果表明，微球的运动距离随微球尺寸的增加而降低。直径约为 40 μm 和 70 μm 时微球运动距离分别约为 795.7 μm 和 43.7 μm。这是因为微球的质量随着尺寸的增加而增加，导致微球与基质表面的阻力增大，进而在实验过程中观察到微球的运动距离降低[图 3(a)～(d)]。

此外，对微球的推进效率进行研究。从图 3(a)～(b)中观察到微球的运动距离随着激光能量的增加而增加，但是并不意味微球的推进效率升高。为此，引入能够描述微球推进效率的参数——冲量耦合系数 $C_m=mv/E$，定义为微球获得动量与激光能量的比值。实验结果表明，随着激光能量的增加，C_m 数值呈现出先上升后下降的趋势，在能量约为 8 μJ 时，C_m 达到最大值，约 7.1×10^{-7} Ns/J[图 3(e)]。

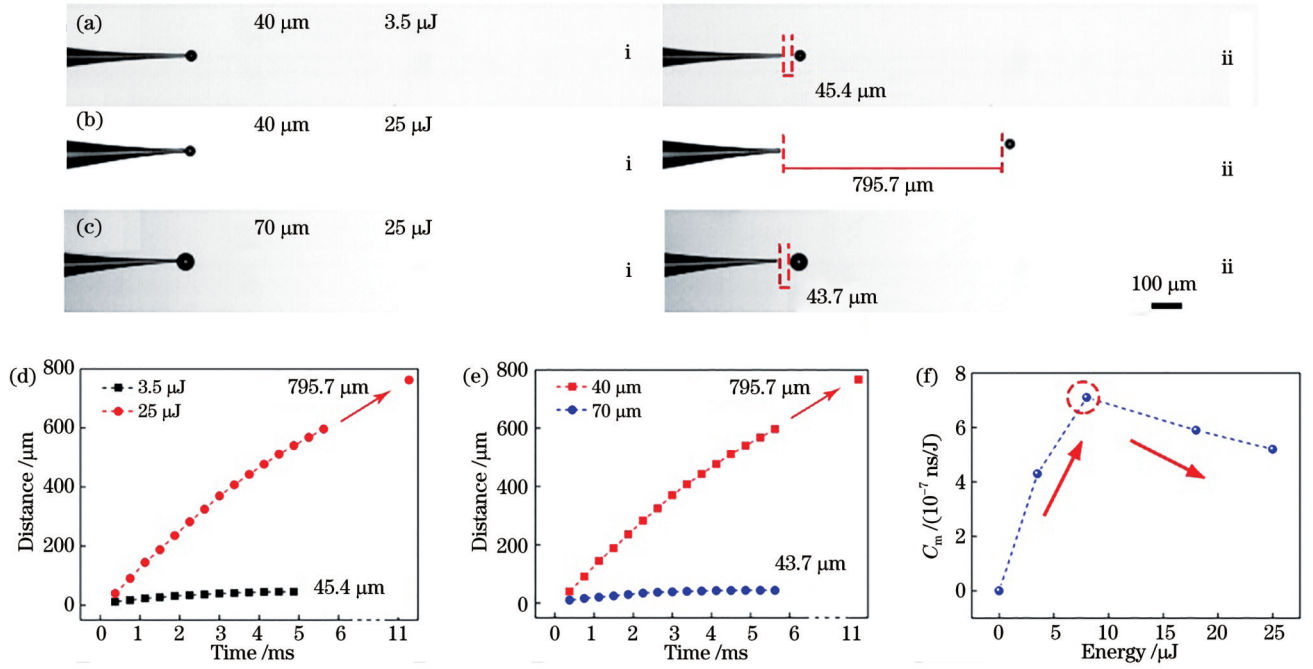

图 3　激光能量、微球尺寸对微球运动的影响。(a)能量～3.5 μJ，直径～40 μm；(b)能量～25 μJ，直径～40 μm；(c)能量～25 μJ，直径～70 μm；(d)能量～3.5 μJ 和～25 μJ 情况下，微球运动距离图；(e)微球直径～40 μm 和～70 μm 情况下，微球运动距离图；(f) C_m 与激光能量的关系

Fig. 3　Effects of laser energy and microsphere size on microsphere motion. (a) E is ～3.5 μJ and diameter is ～40 μm; (b) E is ～25 μJ and diameter is ～40 μm; (c) E is ～25 μJ and diameter is ～70 μm; (d) image of microsphere motion distance with energies of ～3.5 μJ and ～25 μJ; (e) image of microsphere motion distance with diameters of ～40 μm and ～70 μm; (f) C_m as a function of laser energy

3.3　等离子体形成和光纤尖端损伤

首先，研究了等离子体的形成。激光在光纤端会聚出射，与原子相互作用，使得原子中的电子被激发逃离原子核束缚形成自由电子，自由电子被加速并与其他原子碰撞并产生电子[图 4(a)～(b)]，当电子数目达到一定数值(～10^{16}/cm^3)时，形成高温、高压的等离子体[30]。在本课题组之前的研究中，当激光能量高于 28 μJ 时微球表面开始发生变化[31]。而在本文实验中，

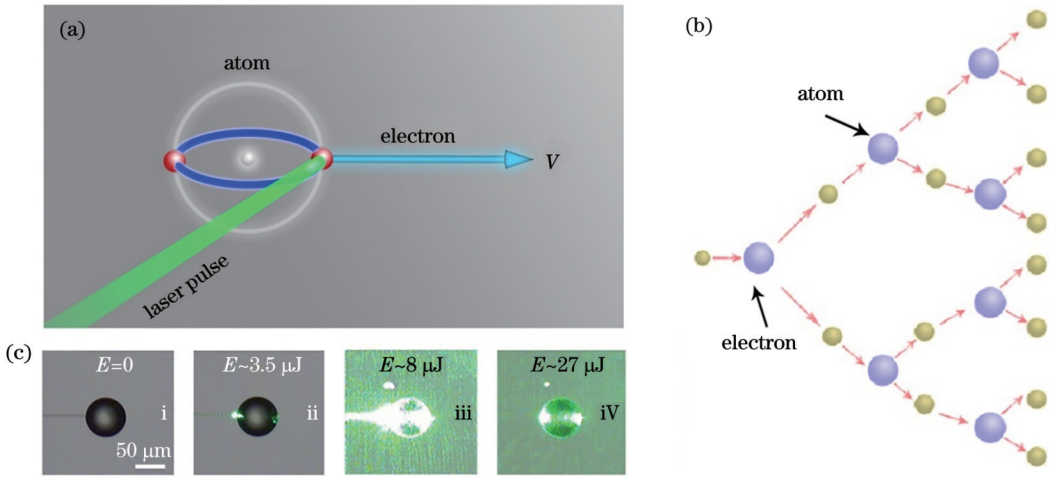

图4　等离子体形成及光纤尖端损伤。(a)高能电子产生;(b)高能电子撞击原子;(c)激光能量对光纤尖端损伤的影响:(i) E=0;(ii) E约为3.5 μJ;(iii) E约为8 μJ;(iv) E约为27 μJ

Fig. 4　Plasma formation and fiber tip damage. (a) Production of high-energy electrons; (b) high-energy electrons colliding with atoms; (c) influence of laser energy on fiber tip damage: (i) E=0; (ii) E is ~3.5 μJ; (iii) E is ~8 μJ; (iv) E is ~27 μJ

光纤尖端出射激光能量均低于28 μJ,所以产生的等离子体为空气等离子体。随后等离子体膨胀形成冲击波通过反冲作用驱动微球前进。

其次,研究了激光能量增加对光纤尖端的损伤。实验结果表明,能量较低(E约为3.5 μJ)时,光纤尖端产生等离子体,大部分能量转移到低密度气体中,用于驱动微球的能量较少。随着激光能量增加(E约为8 μJ),等离子体膨胀形成的冲击波携带能量较高,有利于微球的驱动,同时产生的等离子体会吸收大部分激光能量,即伴随着等离子体屏蔽效应。需要注意的是,激光能量持续上升,超过光纤尖端的损伤阈值时,可以观察到光纤尖端破裂[图4(c)]。

3.4　锥形光纤尖端对出射激光能量、能量密度的影响

为测量光纤尖端直径对出射激光能量、密度的影响,实验中制备了尖端直径为2~125 μm的锥形光纤[图5(a)]。激光电压均匀情况下,光纤尖端出射激光

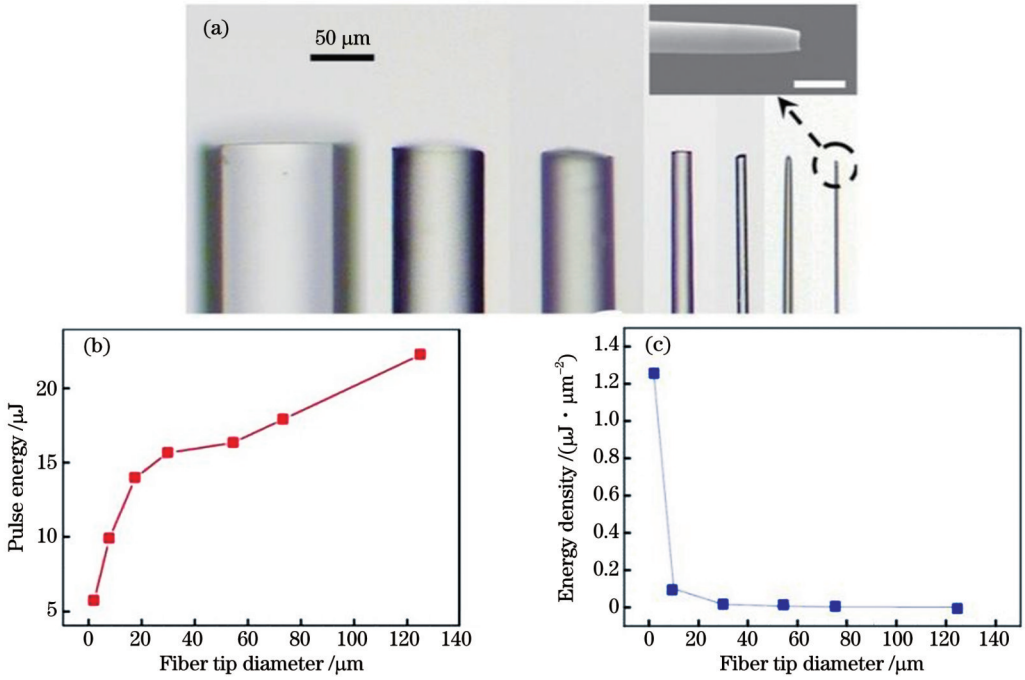

图5　测量不同直径的光纤尖端输出的激光能量。(a)直径2~125 μm的光纤尖端的显微镜图像,其中插图为2 μm光纤尖端的扫描电镜(SEM)图像,比例尺为5 μm;(b)实测脉冲能量与光纤尖端直径的关系;(c)能量密度与光纤尖端直径的关系

Fig. 5　Measurement of laser energy outgoing from fiber tips with different diameters. (a) Microscope image of fiber tips with diameters changing from 2 to 125 μm. Insert is scanning electron microscope (SEM) image of 2 μm fiber tip, and scale bar is 5 μm; (b) relationship between measured pulse energy and fiber tip diameter; (c) relationship between energy density and fiber tip diameter

能量随着尖端直径的增加而增加，归因于散射损耗随光纤尖端直径增大而减小[图5(b)]。而能量密度则表现出相反的变化趋势，这归因于光纤尖端横截面面积的变化。经计算，光纤尖端输出能量密度极限～1.15 μJ/μm^2，而图5(c)中首个数据点能量密度～1.25 μJ/μm^2，该结果表明，此时光纤尖端已经出现损伤。从第二个数据点(能量密度～0.1 μJ/μm^2)开始，能量密度数值骤降，表明尖端直径较小的锥形光纤具有较高的能量密度。

4 结 论

本文提出一种可降低出射激光能量、控制激光光斑大小的锥形光纤结构，并基于该结构实现激光推进微米量级微球，探究了推进机制、微球运动的影响因素。实验中，能量～9.6 μJ的激光从锥形光纤尖端出射，驱动直径～80 μm的微球在6/1000 s内移动了547 μm。由于$P_M \ll P$，说明微球的推进由冲击波弹射机制发挥主导作用，其方式类似于子弹发射。在定性研究激光能量、微球尺寸对微球运动的影响过程中，发现微球的运动距离随着激光能量的增加而增加，随着微球尺寸的增加而降低。分析了光纤尖端出射能量、能量密度与光纤尖端直径的关系，揭示出激光能量呈非线性增加，归因于散射损耗随光纤直径增大而减小。就推进而言，锥形光纤尖端射出的激光表现出低能量，且传播距离较长。本文实验中观察到的光-微球相互作用可能为未来在微观水平上操纵胶体和生物物质的研究提供有益的参考。

参 考 文 献

[1] Zheng Z Y, Liang T, Zhang S Q, et al. Ablation of carbon-doped liquid propellant in laser plasma propulsion[J]. Applied Physics A, 2016, 122(4): 317.

[2] Zheng Z Y, Gao L, Gao H, et al. A "comb" structure measurement of a micrometer displacement in laser plasma propulsion[J]. Applied Physics A, 2014, 117(3): 1577-1581.

[3] Mirza I, Bulgakova N M, Tomáštík J, et al. Ultrashort pulse laser ablation of dielectrics: Thresholds, mechanisms, role of breakdown[J]. Scientific Reports, 2016, 6: 39133.

[4] Zhang Y, Lu X, Zheng Z Y, et al. Transmitted laser propulsion in confined geometry using liquid propellant[J]. Applied Physics A, 2008, 91(2): 357-360.

[5] Ahmad E, Nazeer N, Saeed H, et al. Effect of plasma confinement on laser ablation propulsion parameters by using external semi-elliptical cavities for Aluminum and Silver propellants[J]. Physica Scripta, 2023, 98(9): 095016.

[6] Yu C H, Ye J F, Chang H, et al. Experimental research on characteristics of impulse coupling and plasma plume generated by laser irradiating copper target with nanosecond pulsed laser propulsion[J]. Aerospace, 2023, 10(6): 544.

[7] Nazeer N, Younus A, Jamil Y, et al. Plasma confinement using semi-spherical cavities for enhancement of ablative laser propulsion parameters[J]. Applied Physics B, 2022, 128(11): 206.

[8] Yu H C, Cui L G, Zhang K, et al. Effect of a fiber-capillary structure on nanosecond laser pulse propulsion[J]. Applied Physics A, 2018, 124(1): 37.

[9] Kantrowitz A. Propulsion to orbit by ground based lasers[J]. Astronaut Aeronaut, 1972(10): 74-76.

[10] Myrabo L N, Libeau M A, Meloney E D, et al. Pulsed laser propulsion performance of 11-cm parabolic bell engines within the atmosphere[J]. Proceedings of SPIE, 2004, 5488: 450-464.

[11] Klein A L, Bouwhuis W, Visser C W, et al. Drop shaping by laser-pulse impact[J]. Physical Review Applied, 2015, 3(4): 044018.

[12] Zhang N, Zhao Y B, Zhu X N. Light propulsion of microbeads with femtosecond laser pulses[J]. Optics Express, 2004, 12(15): 3590-3598.

[13] 王谦豪, 赵华龙, 杨小君, 等. 飞秒激光多脉冲烧蚀过程中飞秒时间分辨电子状态的观测研究[J]. 中国激光, 2023, 50(24): 2402101.
Wang Q H, Zhao H L, Yang X J, et al. Femtosecond time-resolved electronic states in femtosecond laser multipulse ablation [J]. Chinese Journal of Lasers, 2023, 50(24): 2402101

[14] Demos S G, Negres R A, Raman R N, et al. Mechanisms governing the interaction of metallic particles with nanosecond laser pulses[J]. Optics Express, 2016, 24(7): 7792-7815.

[15] Ashkin A. Acceleration and trapping of particles by radiation pressure[J]. Physical Review Letters, 1970, 24(4): 156-159.

[16] Xin H B, Li Y Y, Liu X S, et al. Escherichia coli-based biophotonic waveguides[J]. Nano Letters, 2013, 13(7): 3408-3413.

[17] Maimaiti A, Truong V G, Sergides M, et al. Higher order microfibre modes for dielectric particle trapping and propulsion [J]. Scientific Reports, 2015, 5: 9077.

[18] Xu R, Xin H B, Li B J. Massive assembly and migration of nanoparticles by laser-induced vortex flows[J]. Applied Physics Letters, 2013, 103(1): 014102.

[19] Brzobohatý O, Karásek V, Šiler M, et al. Experimental demonstration of optical transport, sorting and self-arrangement using a 'tractor beam'[J]. Nature Photonics, 2013, 7: 123-127.

[20] She W L, Yu J H, Feng R H. Observation of a push force on the end face of a nanometer silica filament exerted by outgoing light[J]. Physical Review Letters, 2008, 101(24): 243601.

[21] Brevik I. Comment on "observation of a push force on the end face of a nanometer silica filament exerted by outgoing light"[J]. Physical Review Letters, 2009, 103(21): 219301.

[22] Mansuripur M, Zakharian A R. Theoretical analysis of the force on the end face of a nanofilament exerted by an outgoing light pulse[J]. Physical Review A, 2009, 80(2): 023823.

[23] Li H Y, Zhang Y D, Li J, et al. Observation of microsphere movement driven by optical pulse[J]. Optics Letters, 2011, 36(11): 1996-1998.

[24] Tong L M, Gattass R R, Ashcom J B, et al. Subwavelength-diameter silica wires for low-loss optical wave guiding[J]. Nature, 2003, 426(6968): 816-819.

[25] Hayakawa T, Ooishi H, Nogami M. Optical bistability of stimulated-emission lines in Sm^{3+}-doped glass microspheres[J]. Optics Letters, 2001, 26(2): 84-86.

[26] 向程江, 刘晓凤, 陶春先, 等. 1064 nm纳秒激光辐照下HfO2/SiO2增透膜损伤的动态过程研究[J]. 中国激光, 2024, 51(8): 0803101.
Xiang C J, Liu X F, Tao C X, et al. Dynamic damage process of HfO_2/SiO_2 anti-reflection coatings under 1064 nm nanosecond laser irradiation[J]. Chinese Journal of Lasers, 2024, 51(8): 0803101.

[27] 付磊, 王萍, 王斯佳, 等. 纳秒脉冲激光诱导的水中双空泡振荡研究[J]. 中国激光, 2022, 49(4): 0407001.
Fu L, Wang P, Wang S J, et al. Dynamics of bubble pairs in water induced by focused nanosecond laser pulse[J]. Chinese Journal of Lasers, 2022, 49(4): 0407001

[28] Brevik I. Experiments in phenomenological electrodynamics and the electromagnetic energy-momentum tensor[J]. Physics Reports, 1979, 52(3): 133-201.

[29] Požar T, Možina J. Observation of microsphere movement driven by optical pulse: comment[J]. Optics Letters, 2012, 37(5): 902.
[30] 葛杨, 李寒阳, 王鸿涛, 等. 激光等离子体爆轰波血栓推进机理的数值模拟研究[J]. 中国激光, 2024, 51(3): 0307204.
Ge Y, Li H Y, Wang H T, et al. Numerical simulation of thrombus propulsion mechanism induced by laser plasma detonation wave[J]. Chinese Journal of Lasers, 2024, 51(3): 0307204.
[31] Yu H C, Li H Y, Wu X, et al. Dynamic testing of nanosecond laser pulse induced plasma shock wave propulsion for microsphere[J]. Applied Physics A, 2020, 126(1): 63.

Microspheres Propelled by Laser Pulses Based on Microfiber Tip

Xing Jiwei, Sun Wenhui, Liu Xuelian, Liu Yanfen, Liu Xiaohua, Liu Xiaojun, Hao Binzheng, Li Jianjun, Luo Wang, Li Qinan, Yu Haichao*

Department of Physics, College of Science, Qiqihar University, Qiqihar 161006, *Heilongjiang, China*

Abstract

Objective The interaction between laser pulses and materials has been extensively studied in recent decades as a common physical mechanism, such as laser propulsion (LP) and laser-induced breakdown spectroscopy. LP has gained widespread attention due to its inherent advantages of reducing launch costs and increasing payload. With the development of LP, the research field has gradually transitioned from macroscopic to microscopic fields. However, during the propulsion process, the direct irradiation of high-energy laser pulses on particles can cause permanent damage to the particle surface, and the large laser spot size can lead to deviations in the particle's trajectory. Therefore, a device that can control the spot diameter and reduce surface damage to particles needs to be proposed. In this work, we propose LP based on a tapered fiber to realize the propulsion of microscale microspheres and analyze the mechanism of LP based on the motion of microspheres. We study the effects of laser energy and microsphere size on the distance of the microsphere. In addition, we analyze the influence of laser energy emitted from the fiber tip on the fiber tip size and discuss the relationship between laser energy density and fiber tip diameter, revealing the nonlinear increase in laser energy and the decrease in scattering loss as the fiber diameter increases. Our research may provide further support for the precise manipulation of colloids and biomaterials at the micrometer level.

Methods 1) Experimental setup for LP. A tapered fiber structure is prepared through flame heating. A Nd∶YAG laser is coupled into the fiber using a 40× objective lens and emitted from the fiber tip. The tip and microspheres are placed on three-dimensional translation stages. By the combination of vertical CCD1 and horizontal CCD2, the driven microspheres can be flexibly and precisely controlled. The dynamics of the microspheres are captured by the CCD1 camera. After the propulsion experiment is completed, the laser energy emitted from the fiber tip is measured by an energy meter. 2) Formation of plasma shock wave. During the interaction between the laser emitted from the fiber tip and the atoms, the electrons in the atoms are excited or transitioned to higher energy states. These high-energy electrons are accelerated and further excite electrons in the atoms. The high-energy electrons collide with other atoms, generating additional electrons. When the number of electrons reaches a certain number ($\sim 10^{16}/\mathrm{cm}^3$), a high-temperature and high-pressure plasma is formed. Subsequently, the shock wave generated by the expansion of the plasma propels the microsphere forward through the recoil effect. 3) Calculation of microsphere movement distance and velocity. The dynamics of the microspheres are recorded by a CCD1 camera with a frame rate of 1000 frame/s. The time interval between adjacent images is 1/1000 s. By analyzing the movement of the microsphere between two images taken at t=1/1000 s as the initial state, the displacement s within the time range of 0-1/1000 s is determined. Then the average velocity $v=s/t$ is calculated. We consider the average velocity as the initial velocity due to the short interaction time between the laser pulse and the microsphere. To reduce experimental errors, the experiment is repeated three times under the same conditions.

Results and Discussions In the experiment of propelling microspheres with a diameter of ~80 μm using a laser with an energy of ~9.6 μJ through a ~8 μm fiber tip, the microsphere moves a distance of 547 μm within a time range of 6/1000 s. The maximum velocity is calculated to be 12.4 cm/s, and the momentum is determined to be $P=8.3\times10^{-11}$ Ns. The calculated value P differs from the theoretical value P_{M} by three orders of magnitude. By adjusting the relative position between the fiber tip and the microsphere, we observe that the microsphere can move in the direction of the fiber as well as diagonally. These findings indicate that the ejection mechanism of shock waves plays a dominant role in the propulsion of

the microspheres (Fig. 2). In the qualitative study of the effects of laser energy and microsphere size on microsphere movement, we find that the movement distance of the microsphere increases with increasing laser energy. It can be explained that with the increase in laser energy, the energy carried by the shock wave formed by the expansion of plasma increases, resulting in a greater force exerted on the surface of the microsphere. On the other hand, as the size of the microsphere increases, the movement distance decreases. This can be attributed to the increased resistance between the microsphere and the substrate surface due to the larger size. The above experimental results further illustrate the propagation characteristics of shock wave (Fig. 3). After investigating the relationship between laser energy and fiber tip diameter [Fig. 5(b)], we discover that the laser energy emitted from the fiber tip exhibites nonlinear increases, which is attributed to declining scattering loss with increasing fiber diameter. The calculated limit of the output energy density at the fiber tip is ~1.15 μJ/μm^2. For a fiber tip diameter of approximately 2 μm, the energy density is ~1.25 μJ/μm^2 [Fig. 5(c)], indicating that the fiber tip has been damaged.

Conclusions We present a straightforward solution that makes LP of microspheres feasible using a tapered fiber structure. In the experiment, a laser with an energy of ~9.6 μJ is emitted from the fiber tip, driving the movement of a ~80 μm diameter microsphere. Within a time range of 6/1000 s, the microsphere moves a distance of 547 μm. The fact that $P_M \ll P$ indicates that the motion of the microsphere is primarily governed by the ejection mechanism of the shock wave, similar to the launch of a bullet. In the qualitative study of the influence of laser energy and microsphere size on microsphere movement, we observe that the movement distance of the microsphere increases with increasing laser energy, while it decreases with increasing microsphere size. We analyze the relationship of pulse energy and energy density with fiber tip diameter, revealing a nonlinear increase in energy, which is attributed to declining scattering loss with increasing fiber diameter. In terms of propulsion, the laser emitted from the fiber tip exhibits the characteristics of low energy and longer propagation distances. The observed interaction between light and microspheres in this experiment may provide valuable insights for future research on manipulating colloids and biomaterials at the microscale.

Key words laser; tapered fiber; plasma; pulse; shock wave